ANALYTICAL BIOCHEMISTRY **263,** 1–12 (1998)
ARTICLE NO. AB982814

Second-Order Kinetic Analysis of IAsys Biosensor Data: Its Use and Applicability

Paul R. Edwards,*,[1] Colin H. Maule,* Robin J. Leatherbarrow,† and Donald J. Winzor‡
Affinity Sensors, Eastbridge House, Bar Hill, Cambridge, CB3 8SL, United Kingdom; †Department of Chemistry, Imperial College of Science, Technology and Medicine, South Kensington, London, SW7 2AY, United Kingdom; and ‡Center for Protein Structure, Function, and Engineering, Department of Biochemistry, University of Queensland, Brisbane, QLD 4072, Australia

Received March 12, 1998

The kinetic analysis of IAsys biosensor association data usually relies upon the assumption of constant ligate concentration. In certain circumstances this assumption may no longer be valid. In a similar vein, the analysis of the dissociation phase assumes the concentration of ligate to be negligible in the liquid phase—an assumption that may not be sustainable for high-affinity interactions. In this paper we derive analytical solutions of the second-order differential kinetic equations for the association and dissociation phases, together with a binding isotherm that also allows for changes in concentration of both the ligand and the ligate. Using these equations it is possible to determine the conditions under which the pseudo-first-order assumption ceases to be valid. It is found that the effect of ligate depletion on the association rate constant becomes significant only when binding low ligate concentrations to ligand on surfaces with high binding capacities or high affinities. Similarly, the rebinding in the dissociation phase is dependent upon the affinity and the ligand capacity together with the starting dissociation response compared to the capacity. Finally, depletion also affects the form of the binding isotherm, particularly in situations involving high matrix capacities for ligate and high-affinity interactions. © 1998 Academic Press

Key Words: **resonant mirror biosensor; protein–protein interaction; second-order kinetics.**

The use of optical biosensors has become widespread for the analysis of both kinetic and equilibrium constants for a variety of interactions (1–3). A general requirement for these biosensors is the covalent immobilization of one of the binding partners to the sensor surface. Its partner, the ligate, is then able to bind to the immobilized ligand from solution, and this binding is monitored in real-time as a change in the refractive index or mass at the sensor surface. Binding data are then routinely fitted to the integrated first-order rate equation below

$$R_t = \frac{R_{max}[A]k_{ass}}{k_{ass}[A] + k_{diss}}(1 - \exp^{-(k_{ass}[A]+k_{diss})t}), \qquad [1]$$

where R_{max} is the ligate binding capacity of the immobilized ligand, [A] is the concentration of ligate, k_{ass} is the association rate constant, and k_{diss} is the dissociation rate constant. The term $k_{ass}[A] + k_{diss}$ is the apparent pseudo-first-order rate constant (k_{on}) with units of s^{-1}. Thus the association and dissociation rate constants can be determined by varying the ligate concentration, [A].

Correct application of this equation requires an effectively constant ligate concentration. This assumption has been questioned for both the Biacore (4) and IAsys (5, 6) instruments. In principle, depletion of the ligate concentration in the liquid phase as the result of binding to the sensor surface is inevitable in the IAsys instrument because of its closed-system design (5, 6). This feature was illustrated (6) by the examination of two systems for which time courses of ligate binding were simulated by numerical integration of the second-order rate equation that allows for depletion of the ligate concentration. In order to explore the effect two binding capacities were used: one corresponding to 625 arc s on the single-channel IAsys instrument, and the other to an extremely high capacity corresponding to 3750 arc s based on the calibration factor of 200 arc s per ng/mm^2 for a sensor-surface area of 16 mm^2 (7). As might reasonably have been expected, the severe capacity led to large errors in the association and dissociation rate constants determined by pseudo-first-order analysis (Eq. [1]). However,

[1] To whom correspondence should be addressed.

0003-2697/98 $25.00
Copyright © 1998 by Academic Press
All rights of reproduction in any form reserved.

for the system with the lower capacity the extent of depletion was insufficient to affect the validity of the pseudo-first-order approximation, whereupon its application led to the return of the input kinetic parameters.

On the basis of a similar pseudo-first-order kinetic approximation during desorption from the sensor surface (ligate concentration is constant and equal to zero), results for this stage may be interpreted in terms of the expression

$$R_t = R_0(\exp^{-k_{diss}t}), \quad [2]$$

where R_0 is the response at the commencement of dissociation by the introduction of buffer into the cuvette. By means of simulations based on second-order kinetics for the system with the higher capacity (6), Eq. [2] was shown to provide an unacceptable description of a high-affinity system (dissociation equilibrium constant, K_D, of 100 nM) but an acceptable description of one with weaker binding (K_D of 10 μM).

Because the selected capacity of 3750 arc s greatly exceeds the levels of matrix substitution usually employed, the range of affinity and kinetic constants incompatible with measurement on the basis of the pseudo-first-order kinetic approximation needs reassessment. In this paper an analytical solution of the differential equation describing second-order kinetics is derived to allow for the respective effects of depletion and rebinding during association and dissociation phases of an IAsys experiment. Also derived is an expression for characterizing the affinity from the binding isotherm obtained under situations involving significant ligate depletion of the liquid phase. The respective effects of ligate depletion and supplementation of the liquid phase during the association and dissociation phases of the IAsys experiment on the kinetic constants obtained by conventional pseudo-first-order analysis have been investigated under more realistic experimental conditions.

MATERIALS AND METHODS

Materials

All chemicals used were of analytical reagent grade. Phosphate-buffered saline, pH 7.4, containing 0.05% Tween (PBS[2]/T) tablets and bovine α-chymotrypsin (MW = 25,000), were obtained from Sigma Chemical Co. (Poole, UK). Recombinant chymotrypsin inhibitor 2 (CI-2, MW = 9,200) was prepared as described by Jandu *et al.* (8). An amine coupling kit (containing 1-ethyl-3-(3-dimethylaminopropyl) carbodiimide (EDC), *N*-hydroxysuccinimide (NHS), and 1 M ethanolamine, pH 8.5) and IAsys carboxymethyl dextran cuvettes were from Affinity Sensors (Bar Hill, Cambridge, UK).

[2] Abbreviations used: PBS, phosphate-buffered saline; CI-2, recombinant chymotrypsin inhibitor 2; EDC, 1-ethyl-3-(3-dimethylaminopropyl)carbodiimide; NHS, *N*-hydroxysuccinimide.

Methods

Principles of operation of the IAsys biosensor. The operating principles of the IAsys resonant mirror biosensor have been described in detail previously (9). The instrument detects changes in refractive index occurring within the evanescent field (a few hundred nanometers from the surface) when one biomolecule, the ligate, in solution binds to its partner, the ligand, immobilized onto the sensor surface. Generally the immobilized ligand is attached to a surface-bound carboxymethyl dextran matrix extending ~200 nm from the sensor surface. Ligand immobilization and ligate interactions can be followed in real-time with the instrument producing a plot of response, measured in arc seconds, against time. The IAsys instrument is based upon a cuvette system comprising of a sample well and the resonant mirror sensing surface. In the case of the single channel manual system used for the experimental investigation the working volume range is 50–200 μl. The wells for the two-channel manual instrument have a maximum working volume of 80 μl. In this experimental work the ligate volume used was 200 μl at a temperature of 22°C.

The interaction of CI-2 with immobilized chymotrypsin. The immobilization of chymotrypsin to carboxymethyl dextran was performed using EDC/NHS chemistry as detailed by Edwards *et al.* (10) Immobilization of 2.5 mg/ml chymotrypsin resulted in a response, after conditioning with 10 mM HCl, of 1100 arc s. This represents the highest immobilization response for chymotrypsin and gives an ligate binding capacity (R_{max}) of 300 arc s. CI-2 was bound at seven different concentrations spanning 2 to 124 nM for 5 min in PBS/T. After this incubation the CI-2 solution was replaced with PBS/T. The chymotrypsin was regenerated with a 2-min wash with 10 mM HCl.

Modeling of biosensor data. Modeling and data fitting were performed using GraFit (Erithacus Software Ltd., Staines, UK), a commercially available data analysis program. All the modeled data were generated assuming a surface area of 4 mm^2, a ligate volume of 80 μl, and a calibration factor of 200 arc s = 1 ng/mm^2.

Equilibrium. The second-order association equation (Eq. [18] in the Appendix) was used to determine equilibrium responses which would be representative of experimental data from the IAsys at different affinities and binding capacities. This was achieved by the use of a large time value (greater than 5000 s). The resulting data were then fitted to the Langmurian isotherm

$$R_{eq} = \frac{R_{max}[A]}{[A] + K_D}, \quad [3]$$

where R_{eq} is the equilibrium response at a concentration [A] of ligate. The difference between the affinity

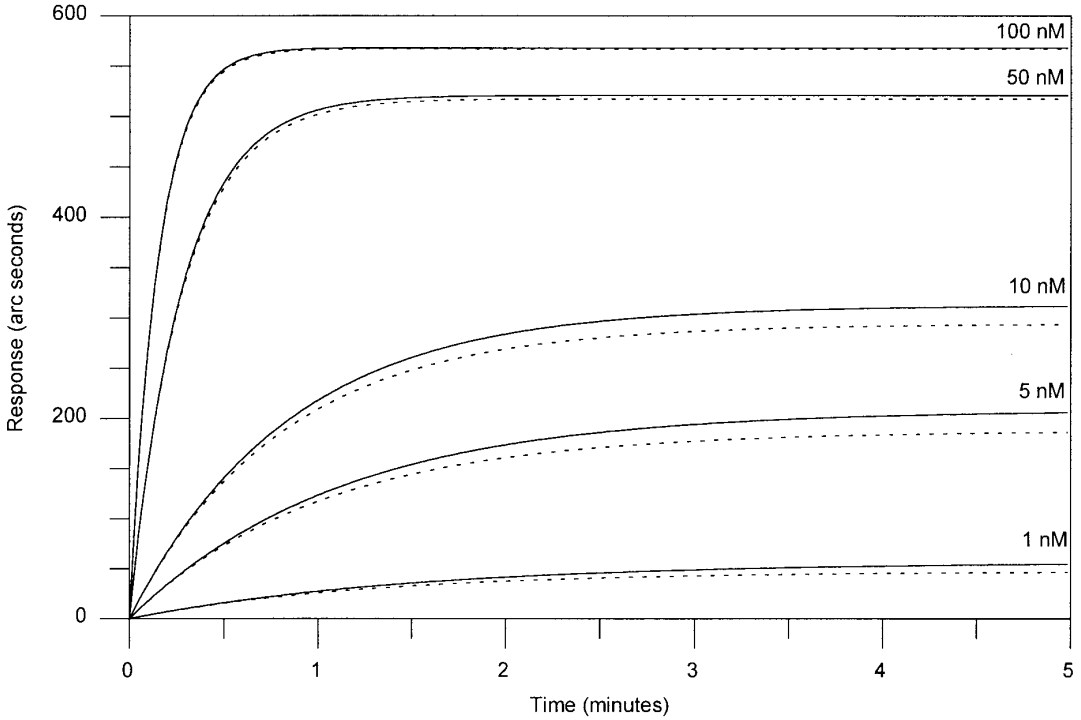

FIG. 1. The effect of ligate depletion upon the IAsys association data. The first-order data (solid line) were generated using Eq. [1] with R_{max} of 625 arc s, a k_{ass} of 1×10^6 M^{-1} s^{-1}, and a k_{diss} of 1×10^{-2} s^{-1}. The ligate concentrations used are shown on the graph. The second-order data (dotted lines) were generated using Eq. [18] with, in addition to the above parameters, a surface area of 4 mm^2, a calibration factor of 200 arc s per ng/mm^2, a volume of 80 μl, and a ligate molecular weight of 50 kDa.

used to generate the data and that returned by the Langmurian isotherm was noted.

Kinetic. Data were generated using the second-order association equation (Eq. [18] in the Appendix). A total of 5 min of association data were generated at 1-s intervals, using various K_D and R_{max} values. Fitting to a first-order equation (Eq. [1]) allowed the apparent pseudo-first-order constant (k_{on}) to be calculated. Plotting this constant against the ligate concentration allowed k_{ass} and k_{diss} to be determined separately. Thus, the effect of ligate concentration, binding capacity, k_{ass}, k_{diss}, and the molecular weight was investigated.

Dissociation data were generated using the second-order dissociation equation and then fitted to the simple exponential dissociation equation (Eq. [2]), with and without an offset parameter. The effect of capacity, individual rate constants, and degree of ligand saturation could be investigated.

Analysis of experimental data. Experimental association data generated using the IAsys instrument for the interaction of CI-2 with immobilized chymotrypsin were fitted using both the first-order and the second-order kinetic analysis. Data with the highest possible level of immobilized chymotrypsin were chosen in an attempt to accentuate the second-order behavior. The experimental isotherm was fitted using the simple Langmurian or the second-order equilibrium equation. The dissociation profiles from the three highest concentrations were fitted to the second-order dissociation equation together with the single exponential dissociation equation with and without an offset.

RESULTS AND DISCUSSION

The general effect of ligate depletion during binding upon the IAsys association data is shown in Fig. 1. These data were modeled with a capacity (R_{max}) of 625 arc s and an affinity of 10 nM ($k_{ass} = 1 \times 10^5$ M^{-1} s^{-1} and $k_{diss} = 1 \times 10^{-2}$ s^{-1}). As expected, the deviation from the first-order equation was more pronounced for longer incubation times and as such the effect on the equilibrium constants will be discussed first.

Equilibrium

As illustrated in Fig. 1 the equilibrium responses are lowered in the event of ligate depletion because the true free concentration is reduced. The proportional effect will be greater at the lower ligate concentrations, as shown by Hall *et al.* (6). The effect of ligate depletion upon the binding isotherm is shown in Fig. 2a,which was generated using a maximum binding capacity of 1250 arc s and an affinity of 1 nM. This high capacity

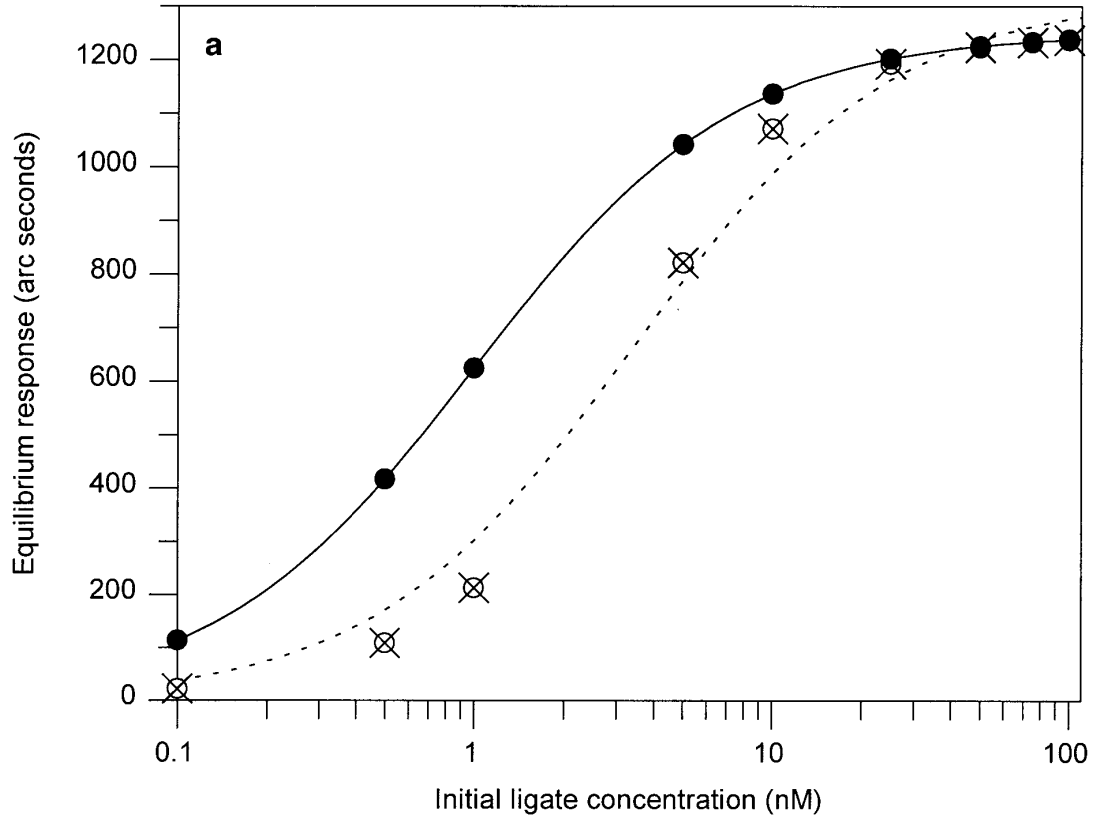

FIG. 2. The effect of ligate depletion upon IAsys binding isotherms. Data were generated using Eqs. [1] (●) and [18] (⊗) over time scales sufficient to allow the determination of equilibrium responses for constant (first-order) and reduced (second-order) ligate concentration, respectively. (a) The isotherm for a 1 nM affinity interaction and R_{max} of 1250 arc s; (b) the isotherm with the same affinity but a lower R_{max} of 200 arc s; and (c) the isotherm for a 10 nM affinity and R_{max} of 200 arc s. Data were fitted to a Langmurian isotherm (Eq. [3]). The solid and dotted curves show the fit to the first- and second-order data, respectively.

was chosen particularly to illustrate the effect upon the isotherm. All data were fitted to a simple isotherm in order to illustrate the effect of depletion on the standard analysis. These data sets illustrate the drop in response due to this depletion. A Langmurian fit to the data is poor, returning an affinity of 3.5 nM. Ligate depletion will be less for many "real" systems that have lower affinity, and/or lower binding capacities. For example, Fig. 2b shows the isotherm generated for a more realistic R_{max} of 200 arc s and an affinity of 1 nM, whereas Fig. 2c shows the isotherm for the same R_{max} but with an affinity of 10 nM. The Langmurian fit to the Fig. 2b data returns an affinity value of 1.4 nM whereas the fit to Fig. 2c returns a value of 10.4 nM.

It is possible to correct for the decrease in ligate concentration arising from binding to obtain accurate affinity values; several options are available. Ligate depletion effects can be accounted for by introducing a simple correction (Eq. [4]), derived from Eq. [3] where $R_{eq} = R_{max}/2$.

$$K_D = K_D^{\text{apparent}} - \frac{R_{max}\beta}{2}. \qquad [4]$$

Here, the affinity determined previously by the Langmurian equation (K_D^{apparent}) is corrected by the incorporation of β (Eq. [14]) which has a value of 5×10^{-12} M/arc s for a 50-kDa ligate, a sensor surface area of 4 mm^2, a volume of 80 μl, and a calibration factor of 200 arc s per ng/mm^2.

The absence of the affinity constant from the correction allows an estimate of the effect of ligate depletion on the measured constant. For Figs. 2b and 2c the correction is 0.4 nM, as expected. This correction scales with the R_{max} value so that the correction for Fig. 2a would be 2.5 nM.

The accuracy of this correction is dependent upon how well the data are described by the Langmurian fit, and thus a more rigorous approach is to correct each of the initial ligate concentrations to allow for ligate depletion. The drop in ligate concentration needed to produce the response, R, can be calculated and used to produce a new equilibrium concentration from Eq. [5].

$$[L]^{\text{eq}} = [L]^{\text{init}} - R\beta. \qquad [5]$$

Correcting each of the data points for ligate depletion lowers the free concentration of ligate plotted. Figure 3

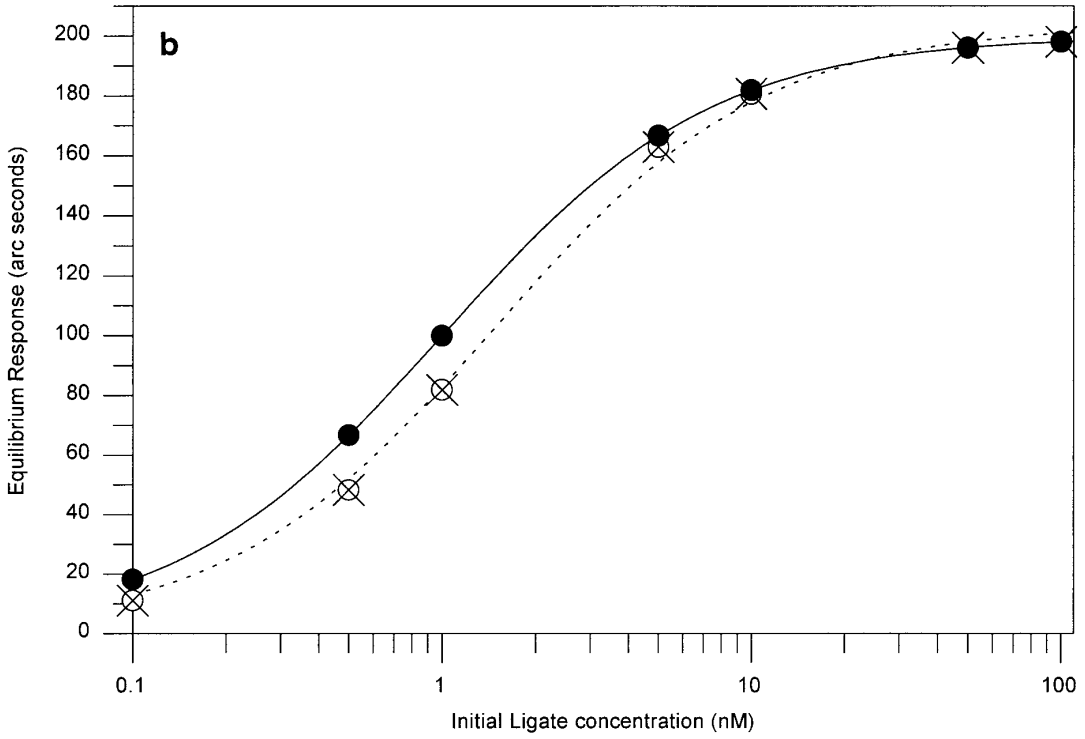

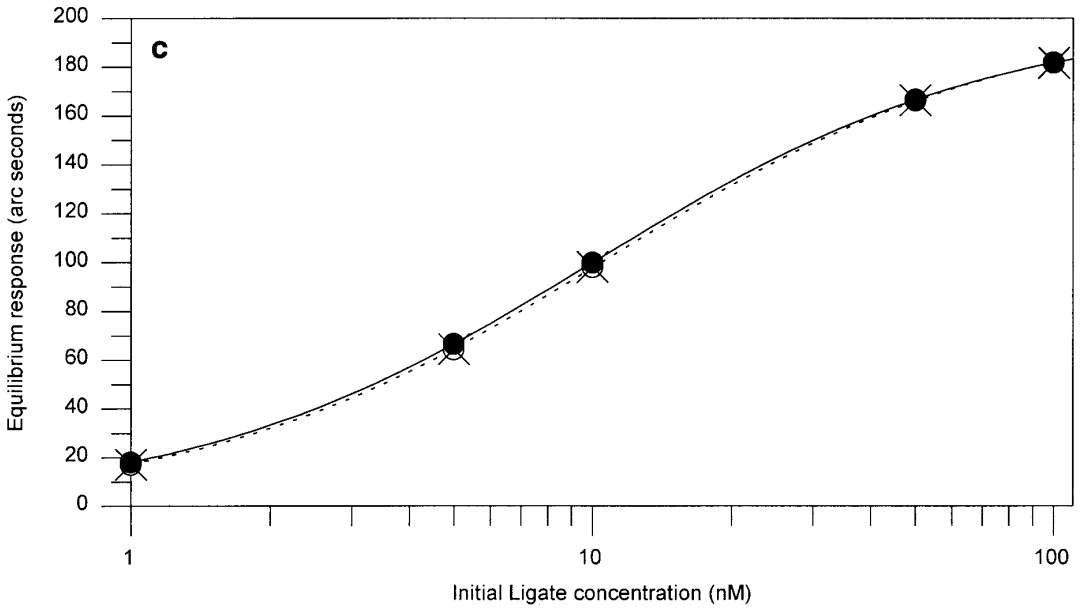

FIG. 2—*Continued*

shows the correction made to the data from Fig. 2a so that all the data points now lie on the Langmurian curve; hence, fitting these corrected data would return the correct affinity of 1 nM.

The third method is to fit the data using the second-order equilibrium equation (Eq. [23]). Figure 4 shows the data from Fig. 2a fitted to this second-order equilibrium equation which gives a 1 nM affinity.

Kinetic

Association data. As noted above, the earlier prediction (6) of severe effects arising from neglect of ligate depletion for a system with a surface capacity (R_{max}) of 3750 arc s and an affinity of 100 nM represents an unrealistic experimental situation. To gain a better insight into the likely consequences of ligate

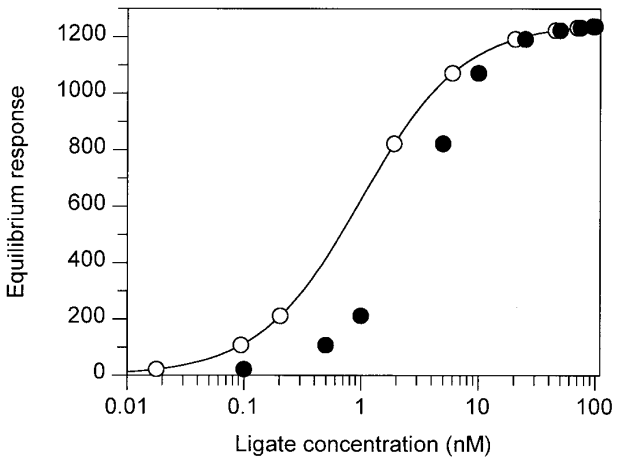

FIG. 3. The effect of correcting ligate concentrations for binding responses upon the isotherm. Data from Fig. 2a are shown as uncorrected data (solid circles). The corrected data (open circles) were obtained by the application of Eq. [5] and the solid line shows the data fitted to a Langmurian isotherm (Eq. [3]).

depletion on the kinetic analysis of a more realistic situation in the new-generation multichannel cuvette, comparable simulation studies have been performed for systems involving a 50-kDa ligate, values of R_{max} in the range 200–1250 arc s, and K_D values of 1–100 nM. On this occasion, however, the time courses of sensor response have been generated by analytical rather than numerical integration of the second-order differential rate equation.

Figure 5 shows the kinetic plot (k_{on} against [ligate]) for an interaction with a 50-kDa ligate having a k_{ass} of 1×10^7 M^{-1} s^{-1} and k_{diss} of 1×10^{-2} s^{-1} over a concentration range of 0.1–100 nM. Ligate depletion is related to the molecular weight of the ligate and the binding capacity, R_{max}. The value of R_{max}/MW was used to normalize the figures, allowing us to relate the effect to any molecular weight ligate. Thus for the example in Fig. 5, a 50-kDa ligate was used; with R_{max} of 1250 arc s, this gives a value of 0.025. The data show that the depletion is worse at lower ligate concentrations and higher binding capacities as is expected. Ligate depletion is observed as an increase in the expected k_{on} at a given concentration, which in turn causes a curvature in the kinetic plot. This curvature is shown in the inset of Fig. 5 over a smaller concentration range. Linear regression analysis of these data would result in an underestimate of k_{ass} and an overestimate of k_{diss}. The influence of R_{max} is also highlighted by the pronounced deviation from that expected (dotted line) at higher loadings to only a small deviation at the lower R_{max} values. Indeed the use of all the data points (0.1–100 nM) results in an error in k_{ass} and k_{diss} of 9 and 50%, respectively, at 0.004, while at the

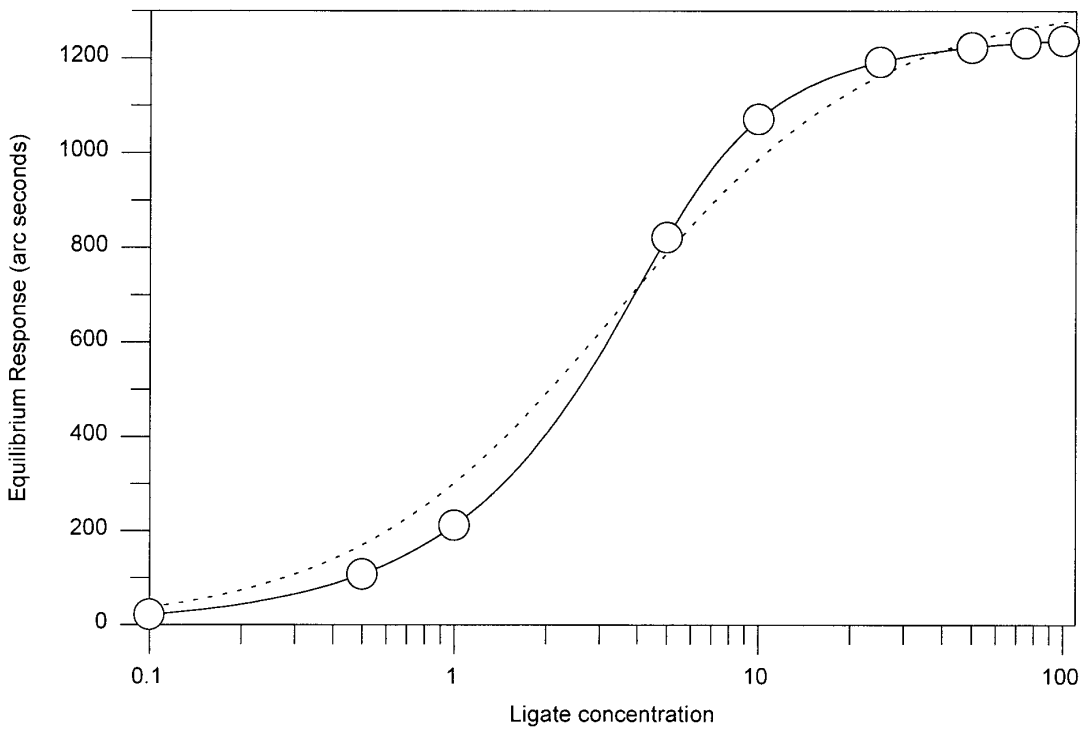

FIG. 4. Binding isotherm showing data from Fig. 2a fitted either to the Langmurian isotherm (Eq. [3]) or to the second-order isotherm (Eq. [23]) shown as dotted and solid curves, respectively.

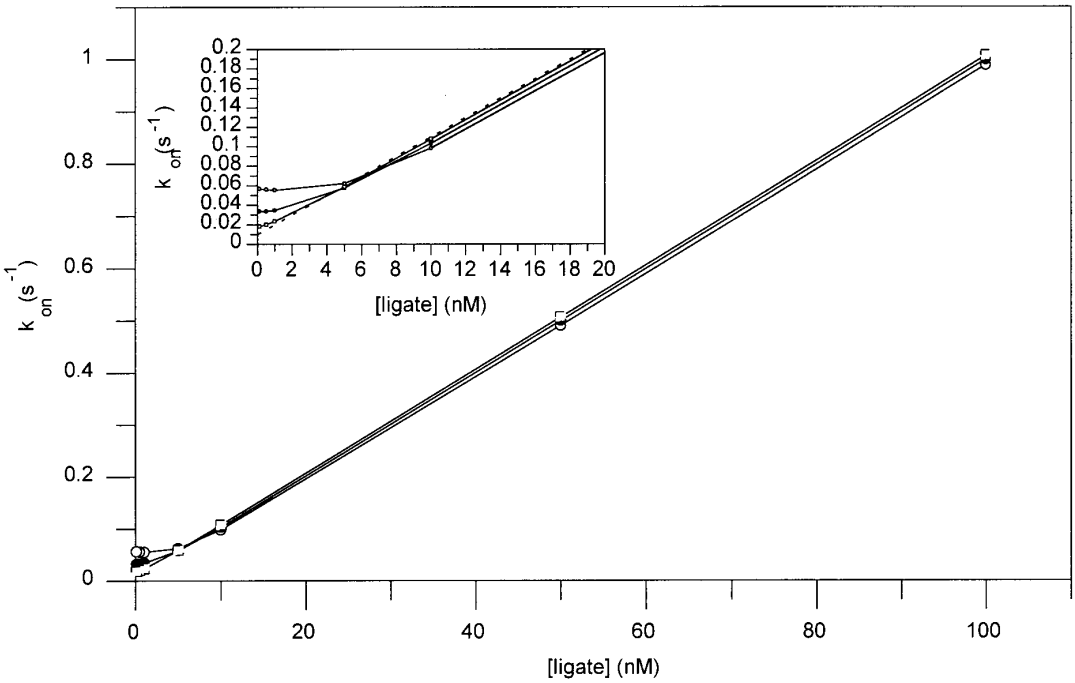

FIG. 5. Kinetic plot (k_{on} against [ligate]) showing the influence of ligate depletion at three R_{max} values for a 50-kDa ligate with a k_{ass} of 1×10^7 M^{-1} s^{-1} and a k_{diss} of 1×10^{-2} s^{-1} over a concentration range of 0.1–100 nM. The values of 0.025 (open circles), 0.0125 (closed circles), and 0.004 (open squares) for R_{max}/MW correspond to maximal responses of 1250, 625, and 200 arc s. The inset shows the same data over the ligate concentration of 0.1–20 nM.

highest capacity (0.025) errors of 60 and 522% are found. Kinetic analysis, however, is often performed at higher ligate concentrations. A typical concentration range might be 1–100 times K_D, which would in the example in Fig. 5 equate to 1–100 nM. Restricting the ligate concentration to 1–100 nM improves the errors dramatically with the k_{ass} and k_{diss} giving errors of 3.7 and 95% on the high capacity surface, respectively.

In a similar manner the kinetic plot for the same interaction as Fig. 5 with the exception of a k_{ass} of 1×10^5 M^{-1} s^{-1} is shown in Fig. 6. The deviation from the expected line is small, with deviations only becoming visible at higher capacities or lower ligate concentrations. The inset of Fig. 6 shows the data between 1 and 20 nM, illustrating the smaller deviations compared to that from the higher k_{ass} (and lower K_D) simulation.

Dissociation data. Analysis of dissociation data via Eq. [2] is based on the assumption that the dissociation of ligate from the sensor surface does not affect the approximation that the ligate concentration in the liquid phase can be regarded as effectively zero. Such an approximation becomes progressively less tenable with increasing reaction affinity because of the ever decreasing concentration at which the rebinding phenomenon becomes significant. Figure 7 shows the dissociation profile over a time scale of 1000 s generated by the second-order dissociation equation (Eq. [22]) with k_{ass} of 1×10^6 M^{-1} s^{-1}, k_{diss} of 1×10^{-2} s^{-1}, a molecular weight of 50 kDa, and an initial dissociation response (R_0) of 300 arc s, with capacities (R_{max}) of 300, 600, 750, and 1000 arc s. Fitting these data with the single exponential dissociation equation without an offset produces a poor fit which becomes worse with increasing capacities. The introduction of an offset value allows the data to be better described for all R_{max} values. Restricting the data to the first 100 s allows the equation without the offset to return values closer to those used for data generation. If the time interval used for the generation of the dissociation data was scaled with the $t_{1/2}$ of the dissociation phase, such that a k_{diss} of 1×10^{-3} s^{-1} data were generated over 1000 s, while 10,000 s of data were generated for a k_{diss} of 1×10^{-4} s^{-1}, then the fit was found to vary with both the affinity of the interaction and the capacity of the ligand. For the dissociation of a 50-kDa protein from a starting response (R_0) of 300 arc s with a capacity of 300 arc s and a K_D of 10 nM, the error in the k_{diss} value determined without an offset was 0.3% compared to the inputted value. Inclusion of an offset term returns a k_{diss} value with an error of 0.8%. For longer dissociation times, the k_{diss} determined without an offset becomes increasingly inaccurate with an error of 2.7% over 1000 s. Over the same time period the inclusion of an offset returns a value with an error of 1.7%. For the same parameters over 100 s but with a 1 nM interaction the error was 22% without an offset and 70.3%

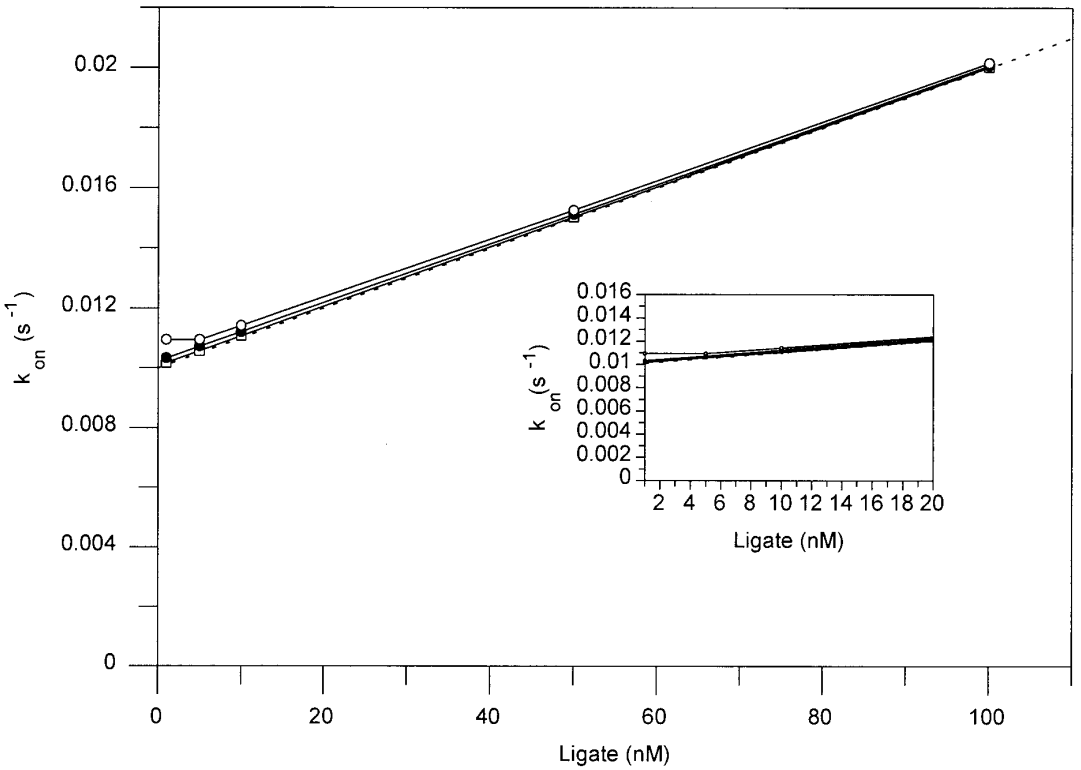

FIG. 6. Kinetic plot (k_{on} against [ligate]) showing the influence of ligate depletion at three R_{max} values for a 50-kDa ligate with a k_{ass} of $1 \times 10^5\ M^{-1}\ s^{-1}$ and a k_{diss} of $1 \times 10^{-2}\ s^{-1}$ over a concentration range of 1–100 nM. The values of 0.025 (open circles), 0.0125 (closed circles), and 0.004 (open squares) for R_{max}/MW correspond to maximal responses of 1250, 625, and 200 arc s. The inset shows the same data over the ligate concentration range of 1–20 nM.

with an offset. Increasing the dissociation time to 1000 s results in errors of 102 and 95.7% for dissociation equations with and without an offset. In all cases the absence of the offset resulted in k_{diss} values which were below the inputted value, whereas the k_{diss} from the offset equation was overestimated. In addition, it was found that the error was increased by decreasing the ratio of R_0/R_{max}. In other words, lowering the response from which the dissociation is initiated increases the likelihood of rebinding due to the increased number of available ligand sites.

Experimental Data Analysis

Association data for the interaction of CI-2 with immobilized chymotrypsin was fitted to both the first-order and second-order association equations. Secondary plots of k_{on} against CI-2 concentration were constructed in order to determine the k_{ass} and k_{diss} values. An immobilization response of 1100 arc s represents the maximum immobilization response for the chymotrypsin and corresponds to an R_{max} value of 300 arc s and thus a corrected value of 300/9200, i.e., 0.032. The influence of depletion upon the determined rate constants was investigated for this biological system at this maximum immobilization response, and the fitted values are given in Table 1. The association rate constant determined from the slope of the k_{on} against CI-2 showed only a small difference between first-order and second-order analysis. From modeling the k_{diss} derived from the intercept would be expected to be more sensitive to depletion. The calculated values show that the second-order analysis gives a lower k_{diss}, as expected. Overall, this results in the derived K_D being lower using the second-order analysis. A similar difference in the affinity constant was observed when allowing for ligate depletion in the isotherm plot. Figure 8 shows the isotherm with the Langmurian fit giving 43.2 ± 9.4 nM, while that of the corrected isotherm gives 33.6 ± 8.5 nM. Once again, allowing for second-order effects results in a lower calculated K_D.

Analysis of the dissociation rate constant of the three highest concentrations from direct application of either the second-order dissociation equation or the dissociation equation with or without an offset revealed that the data were well described by either the second-order or the equation containing the offset. The dissociation of CI-2 (124 nM concentration during binding) is shown in Fig. 9 with the fit to each

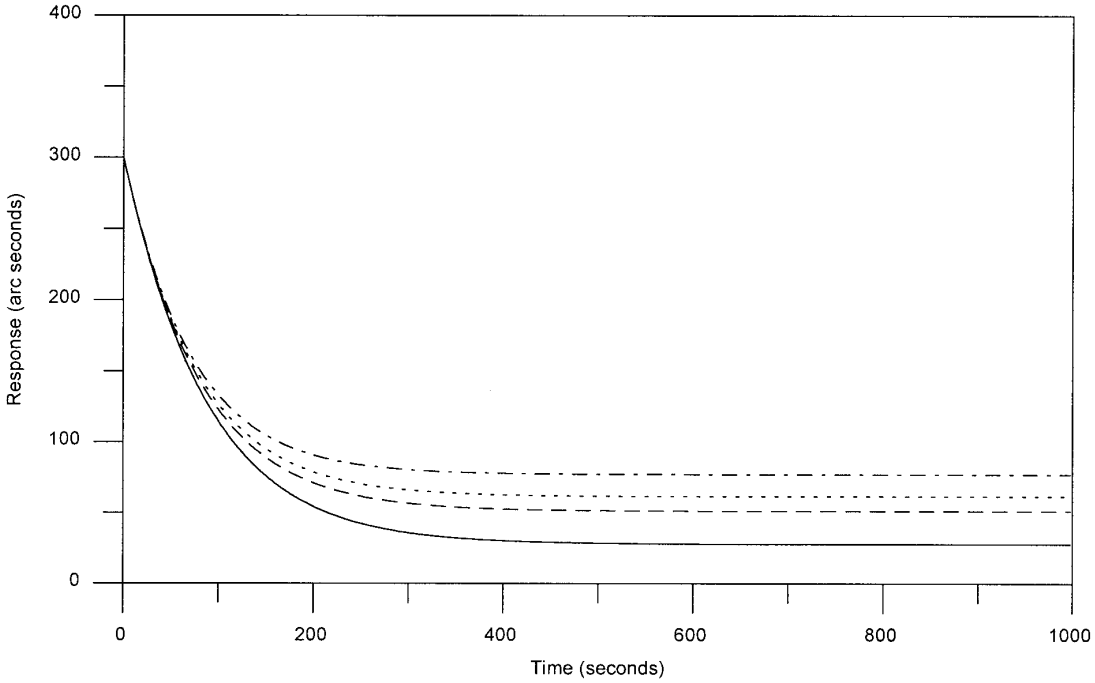

FIG. 7. The effect of binding capacity on the dissociation profile generated by Eq. [22]. R_{max} values of 300 (solid line), 600 (dashed line), 750 (dotted line), and 1000 (dot/dash line) arc s were used together with an initial dissociation response (R_0) of 300 arc s and a K_D of 10 nM.

of the equations also shown. The k_{diss} values derived were $1.44 \pm 0.4 \times 10^{-3}$ s^{-1} for the single exponential equation without an offset, $4.2 \pm 0.1 \times 10^{-3}$ s^{-1} with the offset, and $1.94 \pm 0.03 \times 10^{-3}$ s^{-1} for the second-order equation. Inclusion of the second-order consideration results in a calculated k_{diss} value that is more consistent with k_{diss} derived from the association data.

As a check for internal consistency of the data, the association rate constant was also determined from k_{diss}/K_D. The k_{ass} values so determined were comparable to those obtained from the slope of the plot of k_{on} against ligate concentration and as such provides additional confidence in the analysis.

TABLE 1

Comparison of Rate and Equilibrium Constants Determined by Either First- or Second-Order Analysis of Data from the Interaction of CI-2 with Immobilized Chymotrypsin

	Analysis	
	First-order	Second-order
k_{ass} from kinetic plot (M^{-1} s^{-1})	$7.62\ (0.66) \times 10^{4}$	$7.68\ (0.82) \times 10^{4}$
k_{diss} from kinetic plot (s^{-1})	$2.25\ (0.39) \times 10^{-3}$	$1.87\ (0.48) \times 10^{-3}$
K_D from ratio (nM)	29.5 (5.7)	24.3 (6.7)
K_D from isotherm (nM)	43.2 (9.4)	33.6 (8.5)
k_{ass} from k_{diss}/isotherm K_D	$5.21\ (1.44) \times 10^{4}$	$5.52\ (1.98) \times 10^{4}$

CONCLUSION

As with any closed system, a potential problem in the analysis of IAsys data is the depletion of ligate concentration in the liquid phase during the adsorption stage of the experiment, and its corresponding supplementation during the desorption stage. However, for most interactions measured under normal conditions this effect is small. In the association phase ligate depletion becomes more severe for high-affinity systems binding to an immobilized ligand with a high capacity. One solution to this problem is to work, where possible, at low ligand loadings (10). In cases where this is not practicable, the analysis described in the current paper can be used. Under these conditions it is possible to determine the equilibrium constants either by introducing correction factors or by fitting the data to an isotherm equation allowing for ligate depletion. Kinetic constants determined by pseudo-first-order analysis are also affected by ligate depletion under such conditions, with k_{ass} values being underestimated and k_{diss} values being overestimated. Ligate depletion is readily detected from curvature in the dependence of k_{on} upon ligate concentration, with higher than expected k_{on} values being observed for low ligate concentrations. This curvature is dependent upon the ligand capacity and the affinity of binding. If the curvature is severe the experiment should be repeated with

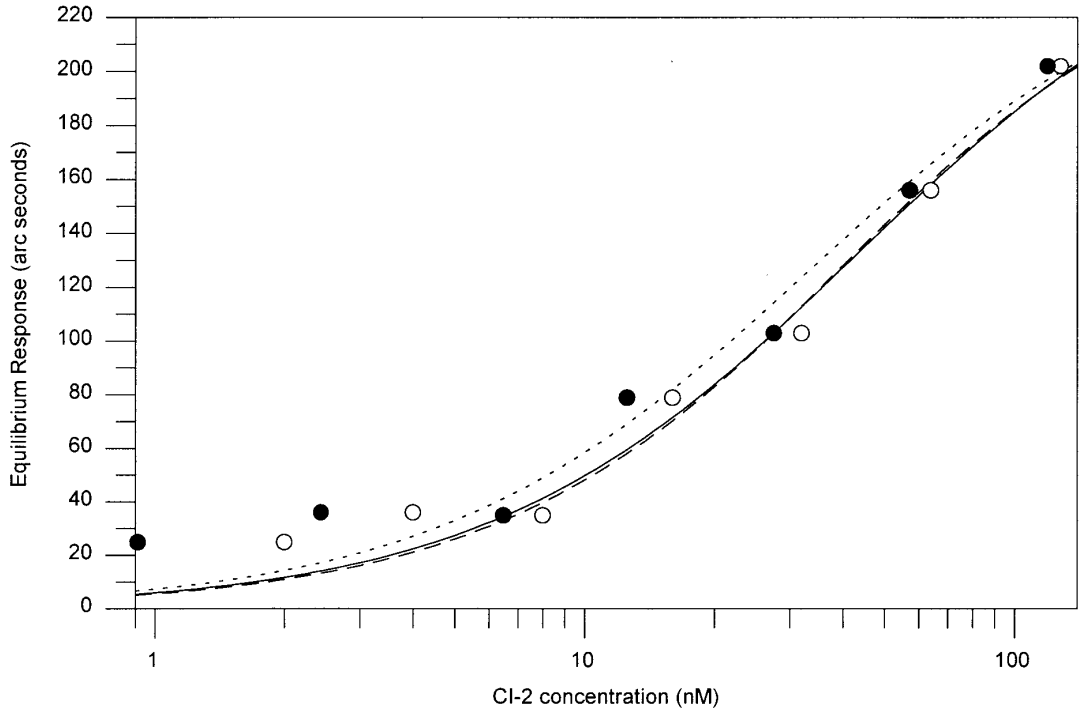

FIG. 8. Isotherm of CI-2 binding to immobilized chymotrypsin. The open circles show the experimental data fitted to a Langmurian isotherm (solid line) or a second-order isotherm (dashed line). Corrected data using Eq. [5] are shown as closed circles fitted to a Langmurian isotherm (dotted line).

lower R_{max} values and higher ligate concentrations in order to avoid the curved region of the plot. The dissociation phase of the ligate may also be complicated by the presence of rebinding which may be observed as incomplete dissociation. This rebinding is more severe with high-affinity systems, high ligand capacity, and dissociation from a low initial response compared to the R_{max}.

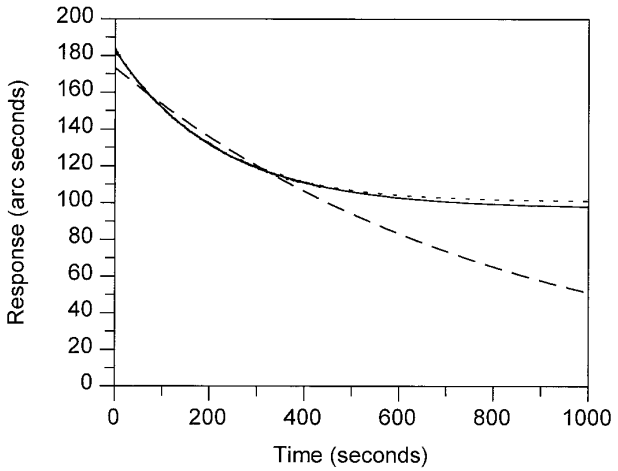

FIG. 9. Dissociation phase for 124 nM CI-2 fitted to single exponential dissociation equations with (solid line) and without (dashed line) an offset, together with a second-order dissociation equation (dotted line).

APPENDIX

Derivation of Second-Order Equations

The reaction between immobilized ligand, B, and ligate, A, from solution is described by Eq. [6],

$$A + B \underset{k_{diss}}{\overset{k_{ass}}{\rightleftharpoons}} AB, \qquad [6]$$

where k_{diss} is the dissociation rate constant and k_{ass} is the association rate constant. The rate of complex formation, AB, is given by Eq. [7].

$$\frac{dAB}{dt} = k_{ass}[A][B] - k_{diss}[AB]. \qquad [7]$$

The instrument response, R, is assumed to be proportional to the concentration of complex, with the initial concentrations of A and B being $[A]_0$ and $[B]_0$, respectively. For a change in instrument response, R/α (g/m^2) must be added, where α is the calibration factor in arc s/g/m^2. During binding, any increase in mass is from molecule A. The number of molecules of A per square meter, for response R, is

$$\frac{R}{\alpha \cdot M_A} \cdot N_A \qquad [8]$$

where M_A is the molecular weight of A and N_A is Avagadros number.

Second-order association equation. If there is a volume V (liter) of ligate and a total surface area S (m^2) on the device then the concentration reduction giving a response R is

$$\frac{S \cdot R}{\alpha \cdot M_A V}. \quad [9]$$

The concentration of A in the cuvette, allowing for a binding response R, is therefore:

$$A(R) = [A]_0 - \frac{S \cdot R}{\alpha \cdot M_A V}. \quad [10]$$

The concentrations of B and AB for a response R are given by

$$B(R) = [B]_0\left(1 - \frac{R}{R_{max}}\right) \quad [11]$$

and

$$AB(R) = \frac{[B]_0 R}{R_{max}}, \quad [12]$$

where R_{max} is the maximal response when all immobilized B sites are filled.

Inserting Eqs. [10–12] into Eq. [7] gives

$$\frac{dR}{dt} = k_{ass}\beta\left\{R^2 - \left(\frac{[A]_0}{\beta} + R_{max} + \frac{k_{diss}}{\beta k_{ass}}\right)R + \frac{[A]_0}{\beta}R_{max}\right\}, \quad [13]$$

where $$\beta = \frac{S}{\alpha \cdot M_A V}, \quad \text{or} \quad [14]$$

$$\frac{dR}{dt} = k_{ass} \cdot \beta(p - R)(q - R); \quad [15]$$

p and q are the roots of the quadratic equation such that

$$R^2 - \left(\frac{[A]_0}{\beta} + R_{max} + \frac{k_{diss}}{\beta k_{ass}}\right)R + \frac{[A]_0}{\beta}R_{max} = 0. \quad [16]$$

This has the general solution of

$$t = \frac{1}{k_{ass} \cdot \beta \cdot (p - q)} \ln \frac{q(p - R)}{p(q - R)} + T, \quad [17]$$

where T is determined by the relevant boundary conditions. At $t = 0$, $R = 0$, which implies that $T = 0$.

Rearranging to give R in terms of t,

$$R = q\left(1 - \frac{p - q}{pE(t) - q}\right), \quad [18]$$

where $E(t) = \exp(k_{ass}\beta(p - q)t)$.

By inspection, q is the equilibrium response at a given ligate concentration.

Second-order dissociation rate equation. The concentration of A in the cuvette during dissociation is given by

$$A(R) = \frac{-S(R - R_0)}{\alpha \cdot M_A V} = -\beta(R - R_0), \quad [19]$$

where R_0 is the initial response with $A = 0$ at $R = R_0$. The concentrations of B and AB are given by Eqs. [11] and [12] such that the differential equation defining the rate of complex dissociation with time is

$$\frac{dR}{dt} = k_{ass}\beta\left\{R^2 - \left(R_0 + R_{max} + \frac{k_{diss}}{\beta k_{ass}}\right)R + R_0 R_{max}\right\}. \quad [20]$$

This has the general solution shown in Eq. [17] and again below,

$$t = \frac{1}{k_{ass} \cdot \beta \cdot (p' - q')} \ln \frac{q'(p' - R)}{p'(q' - R)} + T, \quad [21]$$

where p' and q' are solutions to the quadratic equation using boundary conditions $R = R_0$ at $t = 0$; rearranging gives

$$R(t) = \frac{(p'q' - q'R_0)E(t) - p'q' + p'R_0}{(p' - R_0)E(t) - q' + R_0}, \quad [22]$$

where $E(t) = \exp(k_{ass}\beta(p' - q')t)$.

Equilibrium equation. For binding, q is the equilibrium response, and the quadratic solution of q (Eq. [16]) gives the isotherm equation

$$R_{eq} = \frac{([A]_0 + R_{max}\beta + K_D) - \{([A]_0^2 - 2[A]_0 R_{max}\beta + 2[A]_0 K_D + (R_{max}\beta)^2 + 2R_{max}\beta K_D + K_D^2)\}^{1/2}}{2\beta}. \quad [23]$$

ACKNOWLEDGMENT

The authors thank Dr. Maurice Cox of the National Physics Laboratory for the integration of the second-order equation.

REFERENCES

1. Schuck, P. (1997) *Annu. Rev. Biomol. Structure* **26,** 541–566.
2. Ramsden, J. J. (1997) *J. Mol. Recognition* **10,** 109–120.
3. Garland, P. B. (1996) *Q. Rev. Biophys.* **29,** 91–117.
4. Hall, D. R., Cann, R. R., and Winzor, D. J. (1996) *Anal. Biochem.* **235,** 175–184.
5. Hall, D. R., and Winzor, D. J. (1997) *Anal. Biochem.* **244,** 152–160.
6. Hall, D. R., Gorgani, N. N., Altin, J. G., and Winzor, D. J. (1997) *Anal. Biochem.* **253,** 145–155.
7. Edwards, P. R., Gill, A., Pollard-Knight, D. V., Hoare, M., Buckle, P. E., Lowe, P. A., and Leatherbarrow, R. J. (1995) *Anal. Biochem.* **231,** 210–217.
8. Jandu, S. K., Ray, S., Brooks, L., and Leatherbarrow, R. J. (1990) *Biochemistry* **29,** 6264–6269.
9. Cush, R., Cronin, J. M., Stewart, W. J., Maule, C. H., Molloy, J., and Goddard, N. J. (1993) *Biosensors Bioelectronics* **8,** 347–353.
10. Edwards, P. R., Lowe, P. A., and Leatherbarrow, R. J. (1997) *J. Mol. Recognition* **10,** 128–134.